Engineering 6 (2020) 442–448

Contents lists available at ScienceDirect

Engineering

journal homepage: www.elsevier.com/locate/eng

Research
Food Safety and Health—Article

Redesigned Duplex RT-qPCR for the Detection of GI and GII Human Noroviruses

Danlei Liu [a,#], Zilei Zhang [a,#], Qingping Wu [b], Peng Tian [c], Haoran Geng [a], Ting Xu [a], Dapeng Wang [a,*]

[a] Department of Food Science and Technology, School of Agriculture and Biology, Shanghai Jiao Tong University, Shanghai 200240, China
[b] State Key Laboratory of Applied Microbiology Southern China & Guangdong Provincial Key Laboratory of Microbial Culture Collection and Application & Guangdong Open Laboratory of Applied Microbiology & Guangdong Institute of Microbiology, Guangzhou 510070, China
[c] Produce Safety and Microbiology Research Unit, Western Regional Research Center, Agricultural Research Service, United States Department of Agriculture, Albany, CA 94706, USA

ARTICLE INFO

Article history:
Received 29 August 2018
Revised 19 November 2018
Accepted 30 August 2019
Available online 3 March 2020

Keywords:
Human noroviruses
RT-qPCR
Redesign
Primer
Probe
Detection

ABSTRACT

Human noroviruses (HuNoVs) are major foodborne pathogens that cause nonbacterial acute gastroenteritis worldwide. As the tissue-culture system for HuNoVs is not mature enough for routine detection of the virus, detection is mainly dependent on molecular approaches such as reverse transcription polymerase chain reaction (RT-PCR) and reverse transcription quantitative real-time polymerase chain reaction (RT-qPCR). The widely used primers and probes for RT-qPCR were established in the early 2000s. As HuNoVs are highly variant viruses, viral genome mutations result in previously designed primers and/or probes that were perfectly matched working less efficiently over time. In this study, a new duplex RT-qPCR (ND-RT-qPCR) was designed for the detection of genogroup I (GI) and genogroup II (GII) HuNoVs based on an analysis of viral sequences added in the database after 2010. Using long transcribed viral RNAs, the results demonstrate that the sensitivity of ND-RT-qPCR is as low as one genomic copy for both GI and GII HuNoVs. The performance of ND-RT-qPCR was further evaluated by a comparison with the commonly used Kageyama primer/probe sets for RT-qPCR (Kageyama RT-qPCR) for 23 HuNoV-positive clinical samples. All five GI samples were registered as positive by ND-RT-qPCR, whereas only two samples were registered as positive by Kageyama RT-qPCR. All 18 GII samples were registered as positive by ND-RT-qPCR, while 17 samples were registered as positive by Kageyama RT-qPCR. The sensitivity reflected by the quantification cycle (Cq) value was lower in ND-RT-qPCR than in Kageyama RT-qPCR. Our data suggest that ND-RT-qPCR could be a good fit for the detection of current strains of HuNoVs.

1. Introduction

Human noroviruses (HuNoVs) are major causes of nonbacterial gastroenteritis in all age groups worldwide, and are responsible for nearly half of all gastroenteritis cases globally [1,2]. Norovirus (NoV) belongs to *Caliciviridae* and possesses a linear, single-stranded positive-sense RNA genome approximately 7500 nucleotides in length [3]. The genome is divided into three open reading frames (ORFs). The ORF1 codes for non-structural viral proteins include RNA-dependent RNA polymerase (RdRp); the ORF2 codes a major viral capsid protein (VP1); and the ORF3 codes a minor viral structural protein [4]. NoVs are classified into ten genogroups (GI–GX) encompassing more than 40 genotypes, with multiple strains in the same genotype [5]. Viruses with less than 14.1% difference in VP1 are considered to be at the same subtype level (i.e., different strains in the same genotype), those with 14.3%–43.8% difference in VP1 are considered to be at the same cluster level (i.e., different genotypes), and those with 44.9%–61.4% difference in VP1 are considered to be at the same genogroup level [6]. GI and GII NoVs are major causes of acute gastroenteritis in humans [7], with GII.4 being the most common genotype for NoV gastroenteritis worldwide.

Due to the lack of an easy and reliable *in vitro* cultivation method, many other approaches have been utilized for the detection of HuNoVs, including electron microscopy (EM) [8], enzyme-linked immunosorbent assay (ELISA) [9], and molecular approaches such as reverse transcription polymerase chain reaction (RT-PCR) and reverse transcription quantitative real-time polymerase chain reaction (RT-qPCR) [10–12]. Among these, RT-qPCR has been widely used as a gold standard for the detection

* Corresponding author.
E-mail address: dapengwang@sjtu.edu.cn (D. Wang).
# These authors contributed equally to this work.

https://doi.org/10.1016/j.eng.2019.08.018

of HuNoVs due to its high sensitivity and specificity [13–15]. In previous reports, primers were derived from the sequence at the ORF1–ORF2 junction, which is considered to be the most conserved region in the genome of HuNoVs [13,16]. Kageyama et al. [13] reported on the first of such primer/probe sets for GI and GII in 2003. Several similar primer/probe sets for HuNoVs were subsequently reported from 2003 to 2007 [13,16–19]. These sets of primers and probes remain in wide use for the detection of HuNoVs, despite the absence of updates. Due to the RNA nature of noroviral genomes, mutations occur frequently and result in potential mismatches between once-perfectly matched primers/probes and changed viral sequences. In addition, more sequence data is available now than ten years ago, when all these primers/probes for RT-qPCR were developed. An increasing number of strains and genotypes have been discovered with the rapid development of sequencing technology, many of which have been mismatched with the primer/probe sequences designed ten years ago to produce false-negative results. Therefore, it is necessary to redesign new primer/probe sets using an updated sequence database in order to optimize the detection of current strains of HuNoVs. In this study, new genomic sequences of GI and GII HuNoVs that have been identified since 2010 were collected from the GenBank and analyzed by Molecular Evolutionary Genetics Analysis (MEGA) 7.0. Primer/probe sets for GI and GII HuNoVs were redesigned, evaluated, and compared with the prototype Kageyama primer/probe in a set of clinical samples with representative genotypes of HuNoVs.

2. Materials and methods

2.1. Target sequence collection

A total of 132 new GII HuNoVs complete genomes that have been added since 2010 were retrieved from the National Center for Biotechnology Information (NCBI)[†] on 1 May 2018. As there were few new complete sets of genomic data within GI, all complete sequences of GI (a total of 57) were retrieved from the NCBI on 1 May 2018 and were aligned to identify the conserved regions for GI according to the method described in Section 2.2. In addition, using a fragment of GI.2 sequence (GenBank No. KF306212.1) 5288–5427 as a template for a Basic Local Alignment Search Tool (BLAST) search, a total of 90 newly added GI partial sequences identified after 2010 and located in the conserved region genome with a high quality of assemblies (a cutoff of 80%) were retrieved from the NCBI.

2.2. Multiple alignments and redesign of primer/probe sets

The complete sequences of GI (57) and GII (132) HuNoVs that were downloaded, as mentioned above, were analyzed with Simplot version 3.5.1 [20] to generate similarity plots and to identify conserved regions used for redesigning new primers and probes. Two strains with a complete genomic sequence, GI.2 (GenBank No. KF306212.1) and GII.6 (GenBank No. KU870455.1), were used as roots in this study. The maximum likelihood (ML) phylogenetic trees of each genogroup were constructed by MEGA 7.0 software[‡] based on 90 (GI) and 132 (GII) newly added (since 2010) sequences located in the conserved region. The reliability of the clustering results was evaluated using a bootstrap test (1000 replications).

After analyzing the conserved regions and the frequency of each nucleotide at each position of the GI and GII HuNoVs, two sets of primers/probes were named as follows: LZIF, LZIR-A, LZIR-B, and LZIP for GI; and LZIIF-A, LZIIF-B, LZIIR, and LZIIP for GII (Table 1).

2.3. Viral RNA extraction from clinical samples

HuNoV-positive clinical samples were kindly provided by Dr. Zhiyong Gao at the Beijing Center for Disease Control and Prevention (CDC), Dr. Ningbo Liao at the Zhejiang CDC, and Dr. Huiying Li at the Chinese CDC. Stool samples were suspended (10%, w/v) in phosphate-buffered saline (PBS, pH = 7.4), vortexed, and centrifuged at 4378 $r \cdot min^{-1}$ for 5 min. The supernatants were stored at −80 °C in aliquots until used.

Viral RNAs were extracted from 140 μL of 10% stool suspension with a HiPure Viral RNA Kit (Magen, China) according to the manufacturer's instructions. RNAs were eluted with 60 μL of RNase-free double-distilled water (ddH_2O) and kept at −80 °C until used.

2.4. In vitro *transcription of RNA as positive controls*

Plasmid DNAs for GI and GII HuNoVs were constructed by amplifying fragments from a GI.5 HuNoV (sample 57565) using the primers GI-4610-F(5′-TGATGCWGAYTATACAGCWTGGGA-3′) and GI-5704R(5′-CATYTTYCCAACCCARCCATTATACAT-3′), and by amplifying fragments from a GII.17 HuNoV (sample 15651202) using P290 [21] and GIISKR [22]. The amplified fragment was 4558–5675 (GenBank No. KF306212.1) for GI and 4298–5383 (GenBank No. KU870455.1) for GII. RT-PCR was carried out in a total volume of 20 μL using the One-Step RT-PCR kit (Takara, China) according to the manufacturer's protocol. Polymerase chain reaction (PCR) products were cloned into the pMD18-T vector (Takara, China). The recombinant plasmids were transfected into *Escherichia coli* TOP10 (GENEWIZ, China). After being double digested by *Hin*d III and *Bam*H I, the fragments were inserted into pET-28a (+) (ThermoFisher, China) under a T7 promotor to create recombinant plasmids pET28-GI-M and pET28-GII-M. The final recombinant plasmids were sequenced by GENEWIZ (China) for confirmation and determination of the orientation of the inserted viral sequence.

The inserted viral DNA was transcribed by a T7 RNA polymerase (Beyotime, China) according to the manufacturer's protocol. The purified RNAs were stored at −80 °C in aliquots.

2.5. One-Step RT-qPCR assay

Reactions of the new duplex RT-qPCR (ND-RT-qPCR) were conducted using a single-tube One-Step RT-qPCR kit (Takara, China) and a CFX96 recycler (Biorad, USA). The redesigned primers and probes were synthesized with modified fluorophores and quenchers (GENEWIZ, China). Each 10 μL reaction mixture was consisted of 5 μL 2 × One-Step RT-qPCR Buffer III (Takara, China), 0.2 μL *Ex*

Table 1
Primers/probes designed in this study to detect GI and GII HuNoVs.

Genotype	Name	Sequence (5′–3′)	Position	Polarity
GI	LZIF	GGAGATCGCRATCTCCTGCCCGA	5323–5344	+
	LZIR-A	CTCYGGTACCAGCTGGCC	5407–5426	−
	LZIR-B	CCTCYGGHACCAGCTGACC	5407–5427	−
	LZIP	HEX–CGTCCTTAGACGCCATCATC ATTTAC–MGB	5349–5374	−
GII	LZIIF-A	GTGGGATGGACTTTTACGTGCCAAG	4971–4995	+
	LZIIF-B	GGTGGMATGGATTTTTACGTGCCCAG	4970–4995	+
	LZIIR	CGTCAYTCGACGCCATCTTCATTCAC	5075–5100	−
	LZIIP	FAM–AGCCAGATTGCGATCGCC–MGB	5048–5065	−

FAM: 6-carboxy-fluorescein; HEX: 5-hexachloro-fluorescein; MGB: minor groove binder.

[†] https://www.ncbi.nlm.nih.gov/.
[‡] https://www.megasoftware.net/.

Taq HS (5 U·μL^{-1}, 1 U = 1 μmol·min^{-1}), 0.2 μL PrimeScript RT Enzyme Mix II, 1.2 μL of RNase-free water, 1 μL mixed primers (primers final concentration 0.8 μmol·L^{-1}), 0.4 μL mixed probes (probes final concentration 0.2 μmol·L^{-1}), and 2 μL sample RNA. The cycling conditions were as follows: 3 min at 42 °C and then 5 s at 95 °C, followed by 40 cycles consisting of 3 s at 95 °C and 7 s at 60 °C. Fluorescence was read at the end of each 60 °C extension step. Thresholds were determined by Bio-Rad CFX96 Manager software with amplification-based threshold determination using the default settings.

2.6. Viral RNA-based standard curves for RT-qPCR

The transcribed viral RNA described in Section 2.4 were quantized using a NanoDrop 2000C spectrophotometer according to the manufacturer's instructions (NanoDrop Technologies Inc., USA) and converted into genome copy numbers. The total numbers of genome copies in the RNAs were calculated as follows: Copy number = [(Concentration of RNAs) (ng·μL^{-1})/(molar mass)] × (6.02×10^{23}). The RNA samples were diluted in a 10-fold dilution series (ranging from 10^0 to 10^6 copies·μL^{-1}). Standard curves of GI and GII HuNoVs were generated by plotting RNA copy numbers versus quantification cycle (Cq). The mean Cq values in repeated experiments were plotted to determine the slope and regression. Coefficient (R^2) values were fitted by Origin 2017. Subsequently, the amplification efficiency (E) was calculated using the following equation: $E = 10^{-1/\text{slope}} - 1$ [23].

2.7. Evaluation of three RT-qPCR assays for the detection of HuNoVs

The ND-RT-qPCR developed in this study was side-by-side compared with the commonly used prototype Kageyama RT-qPCR for the clinical positive samples mentioned in Section 2.3.

In assay A, the ND-RT-qPCR was performed as described in Section 2.5. In assay B, the primers and probes were replaced by those designed by Kageyama et al. [13], while the thermal cycle conditions remained the same as for assay A. In assay C, Kageyama RT-qPCR was performed as described previously, with some modifications [24]. In brief, the RT-qPCR reaction mix consisted of the following: 5 μL 2 × One-Step RT-PCR Buffer III, 0.2 μL *Ex Taq* HS (5 U·μL^{-1}), 0.2 μL PrimeScript RT Enzyme Mix II, 0.4 μL of each 10 μmol·L^{-1} primer (COGIF and COGIR, or COGIIF and COGIIR), 0.2 μL of each 10 μmol·L^{-1} probe (RING1(a)-TP, RING1(b)-TP, or RING2-TP), and 2 μL of RNA. RNase-free ddH_2O was added to each well for a total volume of 10 μL. The thermo-cycling parameters were as follows: 30 min at 42 °C and then 95 °C for 5 min, followed by 40 cycles of 15 s at 95 °C, and 1 min at 56 °C.

Cq 40 was used as the cutoff for negative samples. The Cq values obtained from these different RT-qPCR assays were compared.

3. Results

3.1. PlotSimilarity analyses

PlotSimilarity was conducted to identify the conserved regions for designing primers and probes to detect HuNoVs. Complete genomic sequences for a total of 57 GI and 132 GII HuNoVs were analyzed to identify the conserved regions. The conserved regions with highest similarity were found in the ORF1–ORF2 junction of both GI and GII HuNoVs (data not shown).

3.2. Nucleotide sequences of conserved regions from GI and GII strains

With the aim of designing primers and probes to detect epidemic strains of HuNoVs, the conserved regions corresponding to 5288–5427 of KF306212.1 for GI and 4959–5108 of KU870455.1 for GII were used. Ninety sequences of GI and 132 sequences of GII HuNoVs were used to analyze the frequency of each nucleotide at each position. The A, T, C, and G counts of each position are shown in Figs. 1 and 2. Multiple alignments were performed on each genogroup to identify the conserved fragments in the HuNoV genomes. The primers and probes designed in this study (orange) were compared with those reported by Kageyama et al. [13] (gray). Many positions in the viral genome for the binding of the GI primer/probe had changed, and no longer perfectly matched with those in the Kageyama RT-qPCR. After considering the base mismatches between the current viral strain sequences and the Kageyama assay, new sets of primers and probes for GI and GII HuNoVs were designed and tested while considering melting temperature (T_m) values, GC content, amplification efficiencies, and cross reactions between genogroups.

3.3. Quantitation of HuNoVs

Probes for GI (LZIP) and GII (LZIIP) HuNoVs were labeled with 5-hexachloro-fluorescein (HEX) and 6-carboxy-fluorescein (FAM), respectively, in order to detect both genogroups within one reaction tube. Standard curves and parameters generated by the transcript RNAs of GI and GII using the new RT-qPCR assay are shown in Figs. 3 and 4, respectively. Samples calculated to contain a predicted 0.1 copy of the GI and GII HuNoVs showed no signal.

3.4. Comparison of three RT-qPCR assays for the detection of HuNoVs in clinical samples

The three RT-qPCR assays were compared for the detection of GI and GII HuNoVs in fecal samples (Table 2). Of the 23 HuNoV-positive clinical samples, five were GI HuNoVs and 18 were GII HuNoVs. For GI, 5/5 were detected by assay A, 0/5 by assay B, and 2/5 by assay C. A GI.2, a GI.4, and a GI.5 HuNoV sample could not be detected by Kageyama RT-qPCR. For the two detected GI-positive samples, assay A showed significant lower Cq values than assay C ($P < 0.05$), with an average delta Cq of 10.26 ± 0.24. For GII, 18/18 were detected by assay A, 9/18 by assay B, and 17/18 by assay C. A GII.2 sample, 17151101, was failed in assays B and C. For the positive samples of assay B, the Cq values were 1–10 higher than those of assay A for different samples. Almost all (17 of 18) positive samples detected by assay C had higher Cq values than in assay A, with an average delta Cq of 2.20 ± 0.51. In addition, all positive samples detected by assay B were higher than those detected by assay A, with an average delta Cq of 6.26 ± 0.64.

In this study, all the positive samples were detected by assay A; among these samples, the GI.2, GI.4, and GI.5 HuNoVs could not be detected by the other two assays. Few genotypes of GII and none of GI HuNoVs could be detected by assay B. Overall, assay A could detect HuNoV genotypes with a frequency (100.0%) higher than assay B (39.1%) and assay C (82.6%) (Table 2).

4. Discussion

HuNoVs are one of the leading causes of diarrheal diseases worldwide in all age groups. However, limited information is available about the pathogens due to the lack of an efficient system to culture the viruses *in vitro*. The detection of HuNoVs still predominantly relies on ELISA, RT-PCR, and RT-qPCR [25]. Comparative analysis of these methods for clinical outbreak investigations has estimated their sensitivities as follows: ELISA 17%, RT-PCR 86%, and RT-qPCR 100% [26]. Due to their relatively lower detection limits, RT-PCR and RT-qPCR are the most common approaches for detecting HuNoVs.

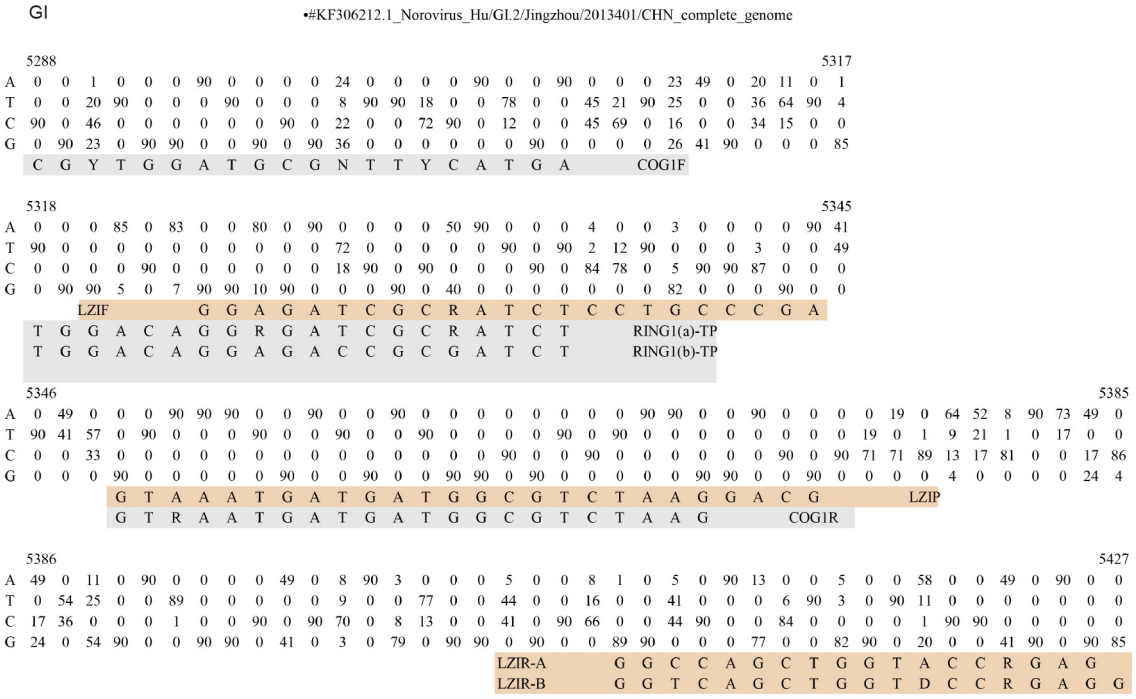

Fig. 1. Multiple alignments of the conserved region of GI HuNoVs.

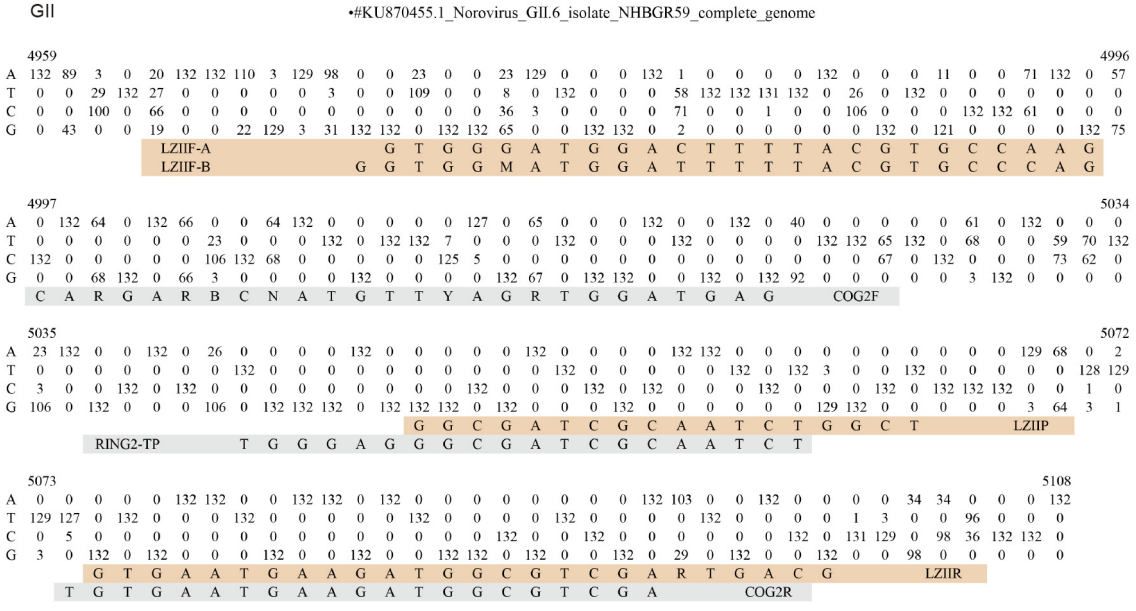

Fig. 2. Multiple alignments of the conserved region of GII HuNoVs.

One-Step RT-qPCR allows for detection and amplification in a single reaction. In general, RT-qPCR is more sensitive than conventional RT-PCR, and is less likely to produce false-positive results due to PCR contamination [25]. Broadly reactive RT-qPCR primer sets for GI and GII HuNoVs have been described by a number of investigators [13,16–19]. Nevertheless, the popular primer sets mentioned here were mainly designed 10–15 years ago, with limited viral sequences available at the time. Moreover, with the ubiquitous presence of mutations in the viral RNA genome, including the highly conserved region, previously designed perfectly matched primers/probes have failed to bind, or bind poorly, to mutated viral genomes. Amarasiri et al. [27] recently redesigned quantitative PCR assays for the genotype-specific quantification of four epidemiologically important genotypes, GII.3, GII.4, GII.6, and GII.17. However, other genotypes of GII and the entire GI were not addressed in their publications. Our study demonstrates the importance of redesigning primers/probes for current strains of GI, as Kageyama RT-qPCR failed in three out of five GI-positive samples tested. Compared with clinical samples, where the overwhelming majority of HuNoV outbreaks are caused by GII strains [28], more frequent detection of GI in food and environmental samples has been reported [29,30].

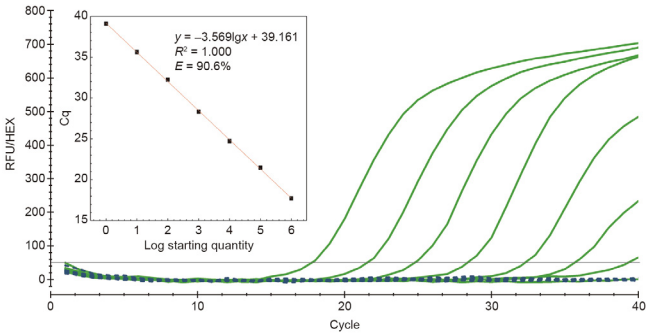

Fig. 3. Standard curve of GI HuNoVs and amplification curve. RFU: relative fluorescence units.

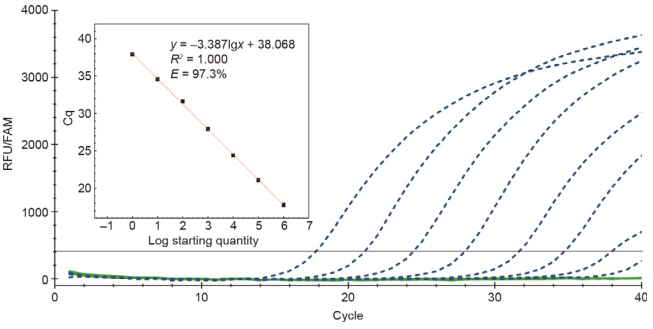

Fig. 4. Standard curve of GII HuNoVs and amplification curve.

Many factors were taken into consideration to design the primers and probes:

(1) **Conservation of selected regions.** Sequences used to design the primers and probes were matched as closely as possible, especially within the 3′ end of primers.

(2) **T_m of primers and probes.** In order to shorten the time for detection assay, annealing and extension were merged into one step at 60 °C, considering the best efficiency of the enzyme. The best T_m for the primers was 60–63 °C and the T_m for probes was 5–10 °C higher.

(3) **Relation between distance and efficiency.** The shorter the distances between the reversed primers and probes, the higher the efficiency of the assay process is.

(4) **Complementary reversal of the probes.** The presence of more guanines than cytosines in the probes can increase the stability of hybridization of the probes; thus, the probes of GI and GII HuNoVs were complementarily reversed.

(5) **Cross reaction of GI and GII HuNoVs.** To avoid a cross reaction between GI and GII virus, the primer/probe sets were redesigned in this study for the simultaneous detection of GI and GII HuNoVs in one tube.

The COG2F primer could be bonded and amplified according to the GI template (data not shown). Therefore, LZIIF primers were not designed according to the sequence of COG2F (the GII primer designed by Kageyama et al.), even though this region is still conservative (Figs. 3 and 4). The perfectly matched primer/probe sequences in the conserved region identified from 90 newly added GI sequences were short, and processed a relatively low T_m value. As both GI and GII will be detected in the same tube in ND-RT-qPCR, TaqMan minor groove binder (MGB) probes were utilized for both GI and GII. The MGB moiety at the 3′ end that increases the T_m of the probe and stabilizes probe–target hybrids can improve the flexibility of probe selection. A 5′ reporter and a 3′ non-photochemical fluorescence quenching (NFQ) were incorporated. The NFQ offers the advantage of lower background signal, which results in better precision in quantitation.

Amplification efficiency is important for the evaluation of the redesigned primer/probe sets. For RT-qPCR, an amplification efficiency between 90% and 110% is considered acceptable [31,32]. In this study, the efficiency of the newly designed primer/probe sets for GI and GII HuNoVs were 90.6% and 97.3%, respectively. The relatively lower efficiency for GI might be caused by three reasons: ① a lack of complete genomic data on GI; ② difficulties in HEX modification, 2′-chloro-7′-phenyl-1,4-dichloro-6-carboxy-fluorescein (VIC) modification is recommended for subsequent

Table 2
Comparison of the performance of three RT-qPCR assays to detect GI and GII HuNoVs in a panel of stool samples positive for HuNoVs.

No.	Sample	Collection time	Genotype	Assay A (Cq value)	Assay B (Cq value)	Assay C (Cq value)
1	57404	Jan 2017	GI.1	18.45 ± 0.37	NA	30.11 ± 0.01
2	14151	Jan 2014	GI.2	32.36 ± 0.66	NA	NA
3	3010	Feb 2014	GI.3	23.38 ± 0.06	NA	32.26 ± 0.04
4	58407	Feb 2017	GI.4	32.66 ± 0.31	NA	NA
5	57565	Jan 2017	GI.5	27.25 ± 0.18	NA	NA
6	17151101	Jan 2017	GII.2	20.98 ± 0.09	NA	NA
7	17152TXZ	Feb 2017	GII.2	27.02 ± 0.01	NA	30.55 ± 0.07
8	15651006	Oct 2015	GII.3	22.69 ± 0.14	NA	25.28 ± 0.24
9	16651029	Oct 2016	GII.4	20.62 ± 0.19	25.54 ± 0.02	22.90 ± 0.62
10	57395	Jan 2017	GII.4	26.48 ± 0.09	36.88 ± 1.67	28.31 ± 0.10
11	17151116	Jan 2017	GII.4	20.79 ± 0.13	28.46 ± 0.05	23.07 ± 0.03
12	58037	Feb 2017	GII.4	29.38 ± 0.07	NA	31.90 ± 0.22
13	C7	Jan 2018	GII.4	15.97 ± 0.21	23.11 ± 0.47	19.27 ± 0.01
14	1704	Nov 2017	GII.4	24.12 ± 0.15	25.61 ± 0.25	24.13 ± 0.26
15	3143	Nov 2014	GII.4	25.69 ± 0.55	NA	28.02 ± 1.15
16	1028	Jan 2014	GII.4	28.91 ± 0.20	NA	30.43 ± 0.53
17	3035	Feb 2014	GII.4	26.35 ± 0.24	NA	27.24 ± 0.74
18	3009	Jan 2014	GII.4	19.09 ± 0.46	NA	23.42 ± 0.45
19	17151030	Jan 2017	GII.6	24.58 ± 0.09	32.09 ± 0.09	26.16 ± 0.09
20	57417	Feb 2017	GII.12	16.26 ± 0.23	24.26 ± 0.01	18.72 ± 0.08
21	1717	Dec 2017	GII.17	19.30 ± 0.41	22.17 ± 0.02	21.54 ± 0.36
22	15651202	Oct 2015	GII.17	29.17 ± 0.13	35.50 ± 1.48	31.18 ± 0.01
23	3014	Jan 2014	GII.PE	23.57 ± 0.30	NA	25.21 ± 0.18
24	NEG			NA	NA	NA

Assay A: ND-RT-qPCR; assay B: primers and probes were replaced with those designed by Kageyama, while the thermal cycle conditions remained the same as for assay A; assay C: Kageyama RT-qPCR. NA: not applicable.

synthesis; ③ a need to further optimize the concentration of primers and probes.

Previous studies have demonstrated that RT-qPCR signals, especially those obtained close to the limit of detection, do not actually originate from the synthesis of target sequences. False-positive results due to PCR artefacts and/or PCR contamination have been reported [33–35]. In some cases, the reduced stringency of primer annealing in the RT-qPCR reverse transcription and amplification steps might lead to non-specific amplification followed by a low level of probe hybridization for a background signal. In this study, the time for each step of the thermal cycles was greatly shortened in order to reduce the chance of non-specific probe hybridization, and the detection time was cut to about 40 min. As suggested in "The MIQE guidelines: Minimum information for publication of quantitative real-time PCR experiments," a Cq greater than 40 was considered to be "positive but not quantifiable" [23], and 40 cycles were considered to be a cutoff in this study.

The sensitivity of ND-RT-qPCR was evaluated by using long viral RNA templates generated in this study. Unlike the standard curves reported previously [17,36,37], where the plasmid DNAs were utilized as templates, two 1500 nucleotides transcribed viral RNAs were used as templates to generate standard curves for GI and GII in this study. The longer transcribed viral RNAs could maintain their secondary structures better than the shorter ones and the plasmid DNAs. The standard curves generated in this study could also reflect the efficiency of the virus RNAs' reverse transcript in the reverse transcript part of the One-Step RT-qPCR detection assay. Using long viral RNAs as templates, the standard curves were generated from 10^0 to 10^6 with R^2 = 1.000. The Cq values were 39.10 and 37.90, respectively, when 10^0 GI and GII were tested. No signals were detected when the viruses were further diluted. The results suggest that the sensitivity of ND-RT-qPCR is 10^0, which is 10 times better than the sensitivity of the Kageyama RT-qPCR assay.

A better performance of ND-RT-qPCR was also observed in the detection of HuNoVs from a set of clinical samples. The ND-RT-qPCR detected GI and GII HuNoVs at the highest frequency (100%). In contrast, lower detection rates were observed when Kageyama RT-qPCR was used for the same set of samples. The Kageyama RT-qPCR worked poorly in the detection of current strains of GI HuNoVs, and failed in three out of five GI samples tested. In this study, the results demonstrated that the primer/probe set designed by Kageyama et al. was not sensitive enough for the detection of the GI HuNoVs in clinical samples. Similar results have been reported by other groups [18,38,39]. The improved sensitivity and amplification efficiency of ND-RT-qPCR was also reflected by the lower Cq values, in comparison with those of the Kageyama RT-qPCR, in each sample tested.

The primers designed in this study were processed at a T_m value of 60–63 °C, which worked perfectly with the temperature of 60 °C that is recommended for annealing and extension in the One-Step RT-qPCR. Therefore, ND-RT-qPCR could be completed in 40 min. To evaluate the primer/probe sets designed by Kageyama et al. in the rapid thermal cycles, assay B was conducted. The results showed that of the five GI samples tested, no positive signal was detected; for GII, nine of the 18 samples were failed by assay B. This result demonstrated that it is not possible for the primer/probe sets designed by Kageyama et al. to be used while compressing the detection time. Based on these results, ND-RT-qPCR can be used to investigate gastroenteritis outbreaks and for disease surveillance. Further studies will evaluate ND-RT-qPCR in the detection of HuNoVs in environmental and food samples (especially in fresh products or shellfish).

In conclusion, our data suggests that ND-RT-qPCR could be a good fit for the detection of current strains of HuNoVs, with its advantages of high sensitivity, specificity, and time efficiency (only 40 min).

Acknowledgements

This work was jointly supported by the Ministry of Science and Technology of China (2017YFC1601200), the National Natural Science Foundation of China (31772078), and the Agri-X Interdisciplinary Fund of Shanghai Jiao Tong University (2017).

Compliance with ethics guidelines

Danlei Liu, Zilei Zhang, Qingping Wu, Peng Tian, Haoran Geng, Ting Xu, and Dapeng Wang declare that they have no conflicts of interest or financial conflicts to disclose.

References

[1] Hall AJ, Wikswo ME, Manikonda K, Roberts VA, Yoder JS, Gould LH. Acute gastroenteritis surveillance through the national outbreak reporting system, United States. Emerg Infect Dis 2013;19(8):1305–9.
[2] Glass RI, Parashar UD, Estes MK. Norovirus gastroenteritis. N Engl J Med 2009;361(18):1776–85.
[3] Jiang X, Graham D, Wang K, Estes M. Norwalk virus genome cloning and characterization. Science 1990;250(4987):1580–3.
[4] Chen H, Wang S, Wang W. Complete genome sequence of a human norovirus strain from the United States classified as genotype GII.P6_GII.6. Genome Announc 2018;6(22):e00489–518.
[5] Chhabra P, de Graaf M, Parra GI, Chan MC, Green K, Martella V, et al. Updated classification of norovirus genogroups and genotypes. J Gen Virol 2019;100(10):1393–406.
[6] Zheng DP, Ando T, Fankhauser RL, Beard RS, Glass RI, Monroe SS. Norovirus classification and proposed strain nomenclature. Virology 2006;346(2):312–23.
[7] Lu QB, Huang DD, Zhao J, Wang HY, Zhang XA, Xu HM, et al. An increasing prevalence of recombinant GII norovirus in pediatric patients with diarrhea during 2010–2013 in China. Infect Genet Evol 2015;31:48–52.
[8] Caul EO, Appleton H. The electron microscopical and physical characteristics of small round human fecal viruses: an interim scheme for classification. J Med Virol 1982;9(4):257–65.
[9] DiCaprio E. Recent advances in human norovirus detection and cultivation methods. Curr Opin Food Sci 2017;14:93–7.
[10] Lees D. International standardisation of a method for detection of human pathogenic viruses in molluscan shellfish. Food Environ Virol 2010;2(3):146–55.
[11] Pang X, Lee BE. Laboratory diagnosis of noroviruses: present and future. Clin Lab Med 2015;35(2):345–62.
[12] Kittigul L, Thamjaroen A, Chiawchan S, Chavalitshewinkoon-Petmitr P, Pombubpa K, Diraphat P. Prevalence and molecular genotyping of noroviruses in market oysters, mussels, and cockles in Bangkok, Thailand. Food Environ Virol 2016;8(2):133–40.
[13] Kageyama T, Kojima S, Shinohara M, Uchida K, Fukushi S, Hoshino FB, et al. Broadly reactive and highly sensitive assay for Norwalk-like viruses based on real-time quantitative reverse transcription-PCR. J Clin Microbiol 2003;41(4):1548–57.
[14] Le Guyader FS, Bon F, DeMedici D, Parnaudeau S, Bertone A, Crudeli S, et al. Detection of multiple noroviruses associated with an international gastroenteritis outbreak linked to oyster consumption. J Clin Microbiol 2006;44(11):3878–82.
[15] Yu Y, Cai H, Hu L, Lei R, Pan Y, Yan S, et al. Molecular epidemiology of oyster-related human noroviruses and their global genetic diversity and temporal-geographical distribution from 1983 to 2014. Appl Environ Microbiol 2015;81(21):7615–24.
[16] Jothikumar N, Lowther JA, Henshilwood K, Lees DN, Hill VR, Vinje J. Rapid and sensitive detection of noroviruses by using TaqMan-based one-step reverse transcription-PCR assays and application to naturally contaminated shellfish samples. Appl Environ Microbiol 2005;71(4):1870–5.
[17] Höhne M, Schreier E. Detection and characterization of norovirus outbreaks in Germany: application of a one-tube RT-PCR using a fluorogenic real-time detection system. J Med Virol 2004;72(2):312–9.
[18] Loisy F, Atmar RL, Guillon P, Le Cann P, Pommepuy M, Le Guyader FS. Real-time RT-PCR for norovirus screening in shellfish. J Virol Methods 2005;123(1):1–7.
[19] Svraka S, Duizer E, Vennema H, de Bruin E, van der Veer B, Dorresteijn B, et al. Etiological role of viruses in outbreaks of acute gastroenteritis in the Netherlands from 1994 through 2005. J Clin Microbiol 2007;45(5):1389–94.
[20] Lole KS, Bollinger RC, Paranjape RS, Gadkari D, Kulkarni SS, Novak NG, et al. Full-length human immunodeficiency virus type 1 genomes from subtype C-infected seroconverters in India, with evidence of intersubtype recombination. J Virol 1999;73(1):152–60.
[21] Jiang X, Huang PW, Zhong WM, Farkas T, Cubitt DW, Matson DO. Design and evaluation of a primer pair that detects both Norwalk- and Sapporo-like caliciviruses by RT-PCR. J Virol Methods 1999;83(1–2):145–54.

[22] Kojima S, Kageyama T, Fukushi S, Hoshino FB, Shinohara M, Uchida K, et al. Genogroup-specific PCR primers for detection of Norwalk-like viruses. J Virol Methods 2002;100(1–2):107–14.
[23] Bustin SA, Benes V, Garson JA, Hellemans J, Huggett J, Kubista M, et al. The MIQE guidelines: minimum information for publication of quantitative real-time PCR experiments. Clin Chem 2009;55(4):611–22.
[24] Tian P, Engelbrektson A, Mandrell R. Two-log increase in sensitivity for detection of norovirus in complex samples by concentration with porcine gastric mucin conjugated to magnetic beads. Appl Environ Microbiol 2008;74(14):4271–6.
[25] Knight A, Li D, Uyttendaele M, Jaykus LA. A critical review of methods for detecting human noroviruses and predicting their infectivity. Crit Rev Microbiol 2013;39(3):295–309.
[26] Fisman DN, Greer AL, Brouhanski G, Drews SJ. Of gastro and the gold standard: evaluation and policy implications of norovirus test performance for outbreak detection. J Transl Med 2009;7(1):23.
[27] Amarasiri M, Kitajima M, Miyamura A, Santos R, Monteiro S, Miura T, et al. Reverse transcription-quantitative PCR assays for genotype-specific detection of human noroviruses in clinical and environmental samples. Int J Hyg Environ Health 2018;221(3):578–85.
[28] Kroneman A, Verhoef L, Harris J, Vennema H, Duizer E, van Duynhoven Y, et al. Analysis of integrated virological and epidemiological reports of norovirus outbreaks collected within the foodborne viruses in Europe network from 1 July 2001 to 30 June 2006. J Clin Microbiol 2008;46(9):2959–65.
[29] Lowther JA, Gustar NE, Powell AL, Hartnell RE, Lees DN. Two-year systematic study to assess norovirus contamination in oysters from commercial harvesting areas in the United Kingdom. Appl Environ Microbiol 2012;78(16):5812–7.
[30] Verhoef L, Vennema H, van Pelt W, Lees D, Boshuizen H, Henshilwood K, et al. Use of norovirus genotype profiles to differentiate origins of foodborne outbreaks. Emerg Infect Dis 2010;16(4):617–24.
[31] Isaksen TE, Karlsbakk E, Repstad O, Nylund A. Molecular tools for the detection and identification of *Ichthyobodo* spp. (Kinetoplastida), important fish parasites. Parasitol Int 2012;61(4):675–83.
[32] Rebrikov DV, Trofimov DY. Real-time PCR: a review of approaches to data analysis. Appl Biochem Microbiol 2006;42(5):455–63.
[33] Stals A, Werbrouck H, Baert L, Botteldoorn N, Herman L, Uyttendaele M, et al. Laboratory efforts to eliminate contamination problems in the real-time RT-PCR detection of noroviruses. J Microbiol Methods 2009;77(1):72–6.
[34] Baert L, Mattison K, Loisy-Hamon F, Harlow J, Martyres A, Lebeau B, et al. Review: norovirus prevalence in Belgian, Canadian and French fresh produce: a threat to human health? Int J Food Microbiol 2011;151(3):261–9.
[35] Stals A, Baert L, Jasson V, Van Coillie E, Uyttendaele M. Screening of fruit products for norovirus and the difficulty of interpreting positive PCR results. J Food Prot 2011;74(3):425–31.
[36] Pang XL, Preiksaitis JK, Lee B. Multiplex real time RT-PCR for the detection and quantitation of norovirus genogroups I and II in patients with acute gastroenteritis. J Clin Virol 2005;33(2):168–71.
[37] Stals A, Baert L, Botteldoorn N, Werbrouck H, Herman L, Uyttendaele M, et al. Multiplex real-time RT-PCR for simultaneous detection of GI/GII noroviruses and murine norovirus 1. J Virol Methods 2009;161(2):247–53.
[38] Van Stelten A, Kreman TM, Hall N, DesJardin LE. Optimization of a real-time RT-PCR assay reveals an increase of genogroup I norovirus in the clinical setting. J Virol Methods 2011;175(1):80–4.
[39] Rupprom K, Chavalitshewinkoon-Petmitr P, Diraphat P, Kittigul L. Evaluation of real-time RT-PCR assays for detection and quantification of norovirus genogroups I and II. Virol Sin 2017;32(2):139–46.